

Antithrombotic drug candidate ALX-0081 shows superior preclinical efficacy and safety compared with currently marketed antiplatelet drugs

Hans Ulrichs,¹ Karen Silence,¹ Anne Schoolmeester,¹ Peter de Jaegere,² Stefaan Rossenu,¹ Jan Roodt,³ Sofie Priem,¹ Marc Lauwereys,⁴ Peter Casteels,⁴ Femke Van Bockstaele,⁵ Katrien Verschueren,⁵ Patrick Stanssens,⁴ Judith Baumeister,¹ and Josefin-Beate Holz⁵

¹Pharmacology Department, Ablynx NV, Zwijnaarde, Belgium; ²Department of Interventional Cardiology, Erasmus Medical Center, Rotterdam, The Netherlands; ³Department of Hematology and Cell Biology, University of Free State, Bloemfontein, South Africa; ⁴Department of Chemistry, Manufacturing and Controls, Ablynx NV, Zwijnaarde, Belgium; and ⁵Clinical Operations Department, Ablynx NV, Zwijnaarde, Belgium

Neutralizing the interaction of the platelet receptor gpIb with VWF is an attractive strategy to treat and prevent thrombotic complications. ALX-0081 is a bivalent Nanobody which specifically targets the gpIb-binding site of VWF and interacts avidly with VWF. Nanobodies are therapeutic proteins derived from naturally occurring heavy-chain-only Abs and combine a small molecular size with a high inherent stability. ALX-0081 exerts potent

activity in vitro and in vivo. Perfusion experiments with blood from patients with acute coronary syndrome on standard anti-thrombotics demonstrated complete inhibition of platelet adhesion after addition of ALX-0081, while in the absence of ALX-0081 residual adhesion was observed. In a baboon efficacy and safety model measuring acute thrombosis and surgical bleeding, ALX-0081 showed a superior therapeutic window compared with marketed anti-

thrombotics. Pharmacokinetic and biodistribution experiments demonstrated target-mediated clearance of ALX-0081, which leads to a self-regulating disposition behavior. In conclusion, these preclinical data demonstrate that ALX-0081 combines a high efficacy with an improved safety profile compared with currently marketed antithrombotics. ALX-0081 has entered clinical development. (*Blood*. 2011;118(3):757-765)

Introduction

The successive adhesion, activation, and aggregation of platelets are key processes in arterial thrombus formation after endothelial damage.^{1,2} Both rupture of atherosclerotic plaques as well as surgical interventions to treat atherosclerosis (eg, percutaneous coronary intervention [PCI]) may cause exposure of the subendothelium and subsequent clot formation. Eventually, this can result in the occlusion of arteries, leading to ischemia, myocardial infarcts, or stroke. Given the central role of platelets in thrombosis, a substantial number of currently marketed antithrombotic drugs, such as aspirin, clopidogrel, and abciximab, target different steps involved in platelet activation and aggregation.^{1,2} Thanks to their complementary mechanisms of action, the combination of these agents inhibits platelet aggregation to a greater extent than either agent alone.³ However, the use of these antiplatelet drugs is hampered by an increased bleeding risk^{1,2} and the occurrence of treatment resistance in some patients.⁴ Moreover, the irreversible nature of their action can complicate the staunching of bleeding.^{1,2}

Inhibition of the initial adhesion of platelets to subendothelial collagen provides an alternative strategy to prevent unwanted clot formation. The plasma glycoprotein VWF plays a pivotal role in this adhesion via binding to exposed collagen on the one hand, and the interaction of its A1 domain with the gpIb-IX-V receptor complex on the surface of platelets on the other hand.⁵⁻⁷ Interestingly, the VWF A1 domain is only exposed under high-shear conditions,^{8,9} so VWF only acts as a bridging molecule between collagen and platelets in small or stenosed arteries. Therefore, it

is expected that drugs inhibiting this interaction between VWF and platelets show an improved safety profile with respect to bleeding tendency. Indeed, the antithrombotic effect of several compounds targeting the gpIb-VWF-A1-axis, like aurointra-carboxylic acid,¹⁰⁻¹² recombinant VWF fragments,^{10,13-16} a recombinant gpIb chimeric protein,^{17,18} anti-VWF mAbs,¹⁹⁻²⁷ and an anti-VWF aptamer²⁸ has been demonstrated in vitro and in vivo, without increasing the bleeding risk.^{13,16-18,21,23,25,28,29} Nevertheless, until now only 3 drug candidates have been evaluated in humans, including ALX-0081.³⁰⁻³³

We developed ALX-0081, a bivalent humanized Nanobody directed against the A1 domain of VWF. Nanobodies are therapeutic proteins derived from the heavy-chain variable domains (VHH) that occur naturally in heavy-chain-only Igs of *Camelidae*.^{34,35} Here we describe the in vitro and in vivo results obtained with ALX-0081. First of all, we optimized its VWF-binding potency by generating a bivalent molecule. Next, we examined the capacity of ALX-0081 to inhibit in vitro platelet aggregation under high-shear conditions and in blood samples from patients with acute coronary syndrome (ACS) undergoing a planned PCI procedure. A baboon model for unstable angina was used to evaluate the in vivo efficacy and safety, reflected by the inhibition of thrombus formation and surgical bleeding, respectively. Finally, the pharmacokinetic (PK) and pharmacodynamic (PD) properties of ALX-0081 were determined in cynomolgus monkey and biodistribution experiments were performed in mice.

Submitted November 9, 2010; accepted April 11, 2011. Prepublished online as *Blood* First Edition paper, May 16, 2011; DOI 10.1182/blood-2010-11-317859.

An Inside *Blood* analysis of this article appears at the front of this issue.

The online version of this article contains a data supplement.

The publication costs of this article were defrayed in part by page charge payment. Therefore, and solely to indicate this fact, this article is hereby marked "advertisement" in accordance with 18 USC section 1734.

© 2011 by The American Society of Hematology

Methods

More details on materials and methods are provided in supplemental Methods (available on the *Blood* Web site; see the Supplemental Materials link at the top of the online article).

Materials

The precursor of ALX-0081 was isolated from a llama immunized with the recombinant A1 domain of VWF and was subsequently humanized, resulting in the monovalent VWF-binding Nanobody PMP12A2h1. ALX-0081 (28 kDa) consists of 2 PMP12A2h1 building blocks, genetically linked to each other with a 3 alanine linker. ALX-0081 was produced in *Escherichia coli* using a secretory system. Under high cell-density fermentation conditions about half of the recombinant protein was found to accumulate in the culture medium. ALX-0081 was further purified from the harvested medium using a process comprising 3 chromatographic steps. A cation exchange resin was used as capture step based on the high isoelectric point of ALX-0081 (experimentally determined pI = 10.4). Supplemental Figure 1 illustrates the high level of purity achieved by this first step. The residual host cell protein level was determined to be ~ 15 ng/mg ALX-0081, while the endotoxin level was found to be 0.01 EU/mg ALX-0081. ALX-0081 was found to be > 99% pure by activity, that is, the major product-related variants were shown to have the same activity as the intended protein.

For experiments in the modified Folts model in baboons, clopidogrel (Plavix, tablets of 75 mg; Sanofi Aventis; Bristol-Meyers Squibb) was pulverized and resuspended in 4.5% methanol. This solution was further diluted in saline and administered intravenously as a slow bolus injection.³⁶ Abciximab (ReoPro, 2 mg/mL; Lilly/Centocor), injectable aspirin (Aspegic, 200 mg/mL; Sanofi), heparin sodium (unfractionated, 5000 IU/mL; Intramed), and epinephrine (1 mg/mL; Intramed) were diluted in vehicle (0.9% NaCl) and administered as an IV bolus injection.

Samples from patients and healthy subjects

To assess the ex vivo efficacy of ALX-0081, blood samples were obtained from 9 ACS patients, elected to undergo a PCI procedure. At baseline (24 hours before the start of the procedure), all but one patient had received aspirin and one patient had also received 600 mg of clopidogrel. A second blood sample was taken 1 hour after the start of the PCI, when all patients had received aspirin, clopidogrel (600 mg), and unfractionated heparin (5000-20 000 U).

Surface plasmon resonance

Experiments were conducted using a Biacore 3000 apparatus and Sensor Chip CM5 (Biacore). Plasma-purified human VWF (CAF/DCF; Belgian Red Cross) or its recombinant A1 domain were immobilized on a CM5 chip until a coupling density of 3500 or 500 response units was reached, respectively. Samples were diluted in HBS-EP buffer (with 0.5M NaCl for the A1-coated chips) and were injected. Dissociation of bound compounds was performed with the same buffer.

Inhibition of ristocetin-induced binding of VWF to platelets

Ninety-six-well microtiter plates (Maxisorp; Nunc) coated with poly-L-lysine (Sigma-Aldrich) were washed and incubated for 1 hour at room temperature (RT) with formalin-fixed human platelets (Dade Behring). Wells were washed and blocked with PBS containing 4% BSA (Sigma-Aldrich). A dilution series of Nanobody was preincubated with 1 µg/mL purified VWF (CAF/DCF; Belgian Red Cross) and 1.5 mg/mL ristocetin (abp) after which the mixture was transferred to the coated 96-well microtiter plate. After 1.5 hours of incubation at 37°C, wells were washed and residual bound VWF was detected with anti-VWF polyclonal Abs, labeled with HRP (DAKO). Ortho-phenylenediamine (Sigma-Aldrich) and hydrogen peroxide were used for visualization. Absorbance was determined

at 490 nm and values were corrected using the absorbance of the respective blanks.

Perfusion chamber experiments

Perfusion experiments were performed with a single-pass perfusion chamber under nonpulsatile flow conditions using a modified small perfusion chamber with a slit height of 0.1 mm and a slit width of 2 mm. Thermanox coverslips (Nunc) were coated overnight with 1 mg/mL human placental collagen type III (Sigma-Aldrich) and subsequently blocked with PBS containing 1% human serum albumin. Five milliliters of blood was incubated with or without ALX-0081 and then circulated through the chamber using an infusion/withdrawal pump (Harvard Apparatus). After the perfusion run, the coverslips were rinsed in HEPES-buffered saline (10mM HEPES, 150mM NaCl, pH 7.4) and platelets were fixed and stained. Platelet deposition on the coverslip was evaluated as platelet surface coverage of 10 randomly chosen pictures using light microscopy (Leitz Diaplan; Leica) and computer-assisted analysis with Optimas 6.0 software (DVS).

Modified Folts model in baboons

Nineteen healthy baboons (*Papio ursinus*) were included in this study. The experimental procedure was modified from the original Folts model in dog³⁷ and from an adapted model in baboon.³⁸⁻⁴⁰

Briefly, a shunt was placed between the femoral artery and femoral vein. It was used for drug administration and blood sampling as well as for monitoring the blood flow with a perivascular ultrasonic flow probe (Transonic Systems). The femoral artery was then injured and external stenosis was applied, resulting in high shear rates and thrombus formation in the femoral artery, and hence a reduction in the blood flow. When blood flow reached almost zero, the thrombus was dislodged. External stenosis was restored, inducing formation of a new thrombus. This repeated process resulted in cyclic flow reductions (CFRs). One CFR is the time between stenosis and complete occlusion of the artery (zero flow). After a control period of reproducible CFRs, the shunt was flushed and saline was administered as an internal control. Subsequently, increasing doses of test item (ALX-0081 [n = 8], abciximab [n = 3], clopidogrel [n = 4], aspirin [n = 3], heparin [n = 3] or saline [n = 2]) were injected as an IV bolus into the shunt. A new injury was applied after inhibition of CFRs to confirm that the inhibition was an effect of the treatment and not of a natural healing phenomenon. After complete inhibition of CFRs after administration of the highest dose of test item, epinephrine (2.2 µg/kg/min) was injected to distinguish between weak and strong inhibitors of the CFRs. Epinephrine alone does not cause platelet aggregation in baboons, but can restore the abolished cyclic flow variations by enhancing the effect of other platelet aggregation factors.⁴¹ Just before each new dose of test item, a surgical bleeding test was performed as described previously.^{38,42,43} Briefly, a 2-cm long and 0.8-cm deep incision was made in the groin and preweighed gauze swabs were inserted. The gauzes were replaced every 30 minutes just before each new dose of test item. The amount of blood loss for each dose was determined by subtracting gauze weight before and after use. Results were expressed relative to the amount of blood loss in the control gauze during the saline injection.

RIPA

Platelet-rich plasma (PRP) was prepared by centrifuging whole blood (180g, 5 minutes). The upper fraction containing the PRP was carefully removed. The lower fraction was further centrifuged at 1500g for 10 minutes to prepare platelet-poor plasma (PPP). Platelets were counted in PRP and diluted in PPP to a final concentration of 200 000 platelets/µL. Ristocetin was added (3 mg/mL; DAKO) and ristocetin-induced platelet aggregation (RIPA) was measured on a platelet aggregometer (Chronolog).

Pharmacokinetics of ALX-0081 in cynomolgus monkey

Twenty-four cynomolgus monkeys (*Macaca fascicularis*) were included in the study. ALX-0081 was administered as an IV bolus injection at 0, 0.02, 0.40, and 8.00 mg/kg. The total active ALX-0081 plasma concentration was

determined via an ELISA. ALX-0081 was captured via a biotinylated bivalent anti-ALX-0081 Nanobody (Abylnx), linked to a neutravidin (Perbio Science; Thermo Fisher Scientific) coated plate. Detection occurred via binding of ALX-0081 to VWF (ZLB Behring; CSL Behring) and subsequent detection via an anti-VWF polyclonal antiserum (DAKO).

Individual plasma concentration-time profiles were subjected to a noncompartmental PK analysis (IV bolus input) using WinNonlin Professional Software Version 5.2 (Pharsight Corporation). Basic PK parameters and associated statistics were calculated.

A mechanistic PK/PD model was developed to simulate plasma concentration time curves of total active drug in nonclinical studies. It consists of 3 compartments (1) free ALX-0081, (2) free VWF, and (3) a VWF-ALX-0081 complex compartment. Total clearance of ALX-0081 was described by elimination of (1) unbound ALX-0081 via renal clearance as a function of the glomerular filtration rate and (2) of ALX-0081 bound to VWF most probably via the liver as a function of circulating VWF plasma levels (defined by synthesis and elimination of free VWF).

RICO

Ristocetin cofactor activity (RICO) was determined using a PAP-8E platelet aggregometer (BioData Corporation). Plasma was prepared by centrifugation of whole blood at 2210g for 15 minutes at RT. Lyophilized platelets (Biopool; Trinity Biotech UK) were diluted according to the manufacturer's instructions and incubated with ristocetin (Biopool, 1 mg/mL final concentration) and plasma. Aggregation was followed for at least 5 minutes. Hemostasis reference plasma (Biopool) was used in 3 different concentrations to set up a standard curve. The percentage of RICO was calculated based on the slopes of the aggregation curves.

Biodistribution of ALX-0081

ALX-0081 was ^{125}I -labeled and administered intravenously in the tail vein of C57Bl6/6J mice either as free Nanobody, or in complex with plasma-purified human VWF. At each indicated time point, 3 mice were bled and subsequently killed to collect different organs (heart, kidneys, liver, lungs, stomach, spleen, and left upper leg). Organs were washed, dried, and weighed. Blood samples and organs were analyzed for the presence of residual radioactivity.

Involvement of human participants or animals

All studies involving human participants or animals reported in this manuscript were approved by the relevant ethical committee or animal care and use committee. All patients and healthy subjects provided informed consent in accordance with the Declaration of Helsinki.

Statistical analysis

For all statistical analyses, variance homogeneity was first evaluated by an F test. Depending on the outcome of the F test, Student *t* tests assuming equal or unequal variances were applied. All tests were 2-sided and a significance level of 5% was used.

Results

The bivalency of ALX-0081 allows tight interaction with its target VWF

As VWF is a multimeric protein, we investigated whether coupling of 2 identical Nanobodies blocking the VWF A1 domain would result in increased binding avidity and hence increased potency. ALX-0081 consists of 2 identical building blocks, PMP12A2h1, genetically fused to each other via a short linker.

The bivalency of ALX-0081 allowed avid binding both to human VWF and to its A1 domain as demonstrated by surface plasmon resonance (Figure 1A-B). PMP12A2h1 clearly showed reversible binding to both VWF and its A1 domain, while a tight

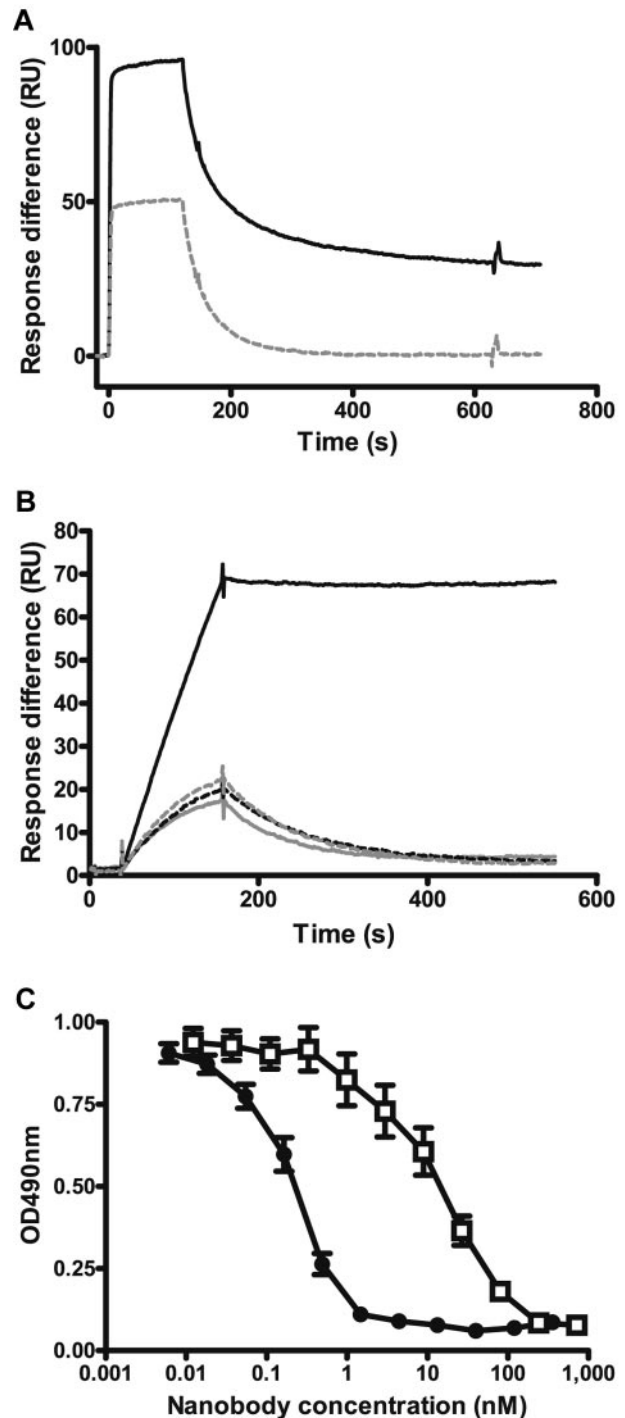


Figure 1. Effect of bivalent Nanobody format on VWF binding. (A) Surface plasmon resonance analysis with a Biacore sensor chip coupled with plasma-purified VWF. Binding and dissociation of 100nM PMP12A2h1 (gray dashed line) and ALX-0081 (black solid line) are shown. (B) Surface plasmon resonance analysis with a Biacore sensor chip coupled with recombinant VWF A1 domain. Binding and dissociation of 1nM PMP12A2h1 (gray dashed line), mock-PMP12A2h1 (gray solid line), PMP12A2h1-mock (black dashed line), and ALX-0081 (black solid line) are shown. Representative of 3 independent experiments. (C) Inhibition of VWF binding to human formalin-fixed platelets: formalin-fixed platelets were bound to poly-L-lysine-coated microtiter plates after which VWF was added in the presence of 1.5 mg/mL ristocetin and different amounts of ALX-0081 (●) or PMP12A2h1 (□). Residual bound VWF was detected colorimetrically. Optical density (OD) measured at 490 nm is shown in function of the Nanobody concentration (mean \pm SEM, $n = 21$).

basically nonreversible interaction was measured for ALX-0081. Binding of ALX-0081 to VWF consisted of monofunctional

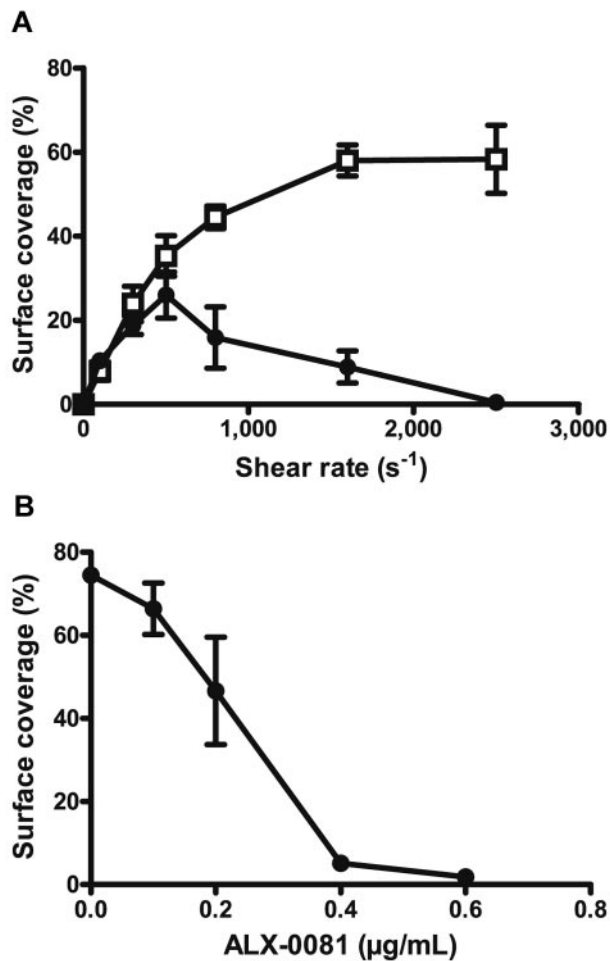


Figure 2. Inhibitory effect of ALX-0081 on in vitro platelet adhesion to collagen type III. Whole blood preincubated with (●) or without (□) ALX-0081 was perfused for 5 minutes over a surface coated with human collagen type III after which the percentage surface coverage was measured. Mean values \pm SEM for 3 independent repeats are shown. (A) Percentage surface coverage in function of shear rate. Concentration of ALX-0081 was 0.8 μ g/mL. (B) Percentage surface coverage in function of ALX-0081 concentration. Shear rate was 1600 s⁻¹.

reversible binding and bifunctional irreversible binding, which could be explained by the spacing of the A1 domains in VWF. Results obtained for equivalents of ALX-0081 in which one of the building blocks was exchanged by an irrelevant, nonbinding Nanobody (PMP12A2h1-mock and mock-PMP12A2h1) confirmed that 2 functional units are required for the described high-affinity interaction (Figure 1B). This avid binding also translated in a more potent inhibition of VWF binding to a platelet surface. Indeed, ALX-0081 showed a significant increase in inhibiting the ristocetin-induced binding of VWF to a platelet surface compared with its monovalent equivalents (Figure 1C). The IC₅₀ of ALX-0081 was 0.26nM \pm 0.04nM compared with 18.46nM \pm 2.75nM for PMP12A2h1 (mean \pm SEM, n = 21) ($P < .0001$), demonstrating a more than 70-fold shift in potency. The IC₅₀ of PMP12A2h1-mock was 20.83nM \pm 5.98nM compared with 0.46nM \pm 0.16nM for ALX-0081 (mean \pm SEM, n = 6) ($P = .019$).

ALX-0081 selectively targets platelet adhesion under conditions of arterial flow

On vascular damage, subendothelial structures are exposed to the blood flow, thereby initiating thrombus formation. Fibrillar colla-

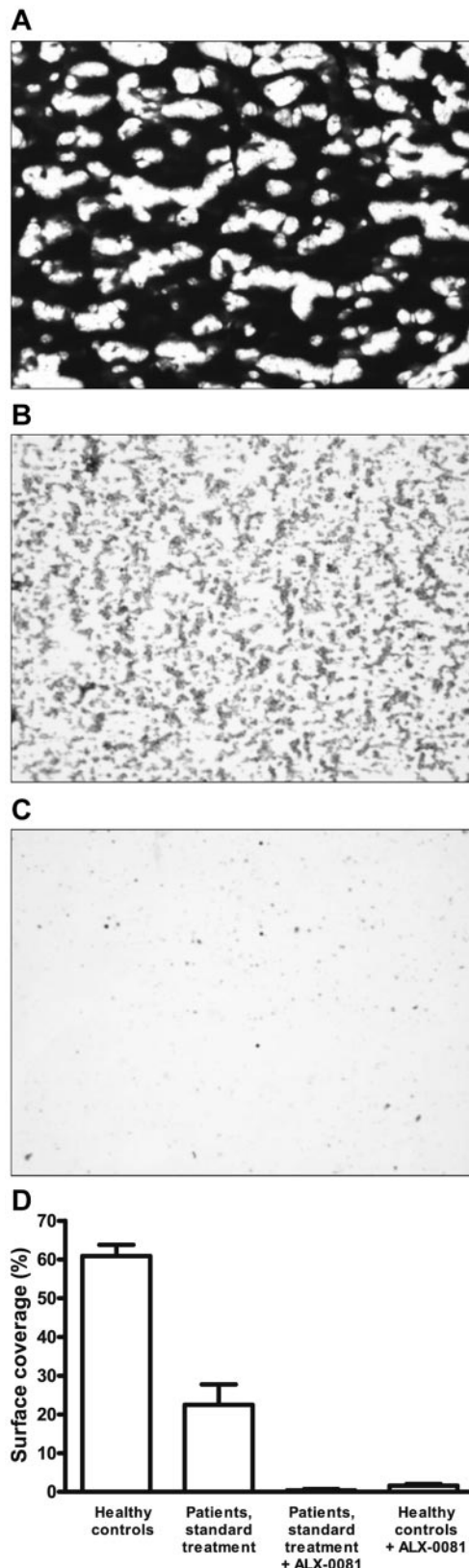


Figure 3. Inhibitory effect of ALX-0081 on ex vivo platelet adhesion to collagen type III. Representative images of platelet deposition on collagen-coated coverslips after perfusion with blood samples from healthy individuals (A) and from PCI patients receiving standard antithrombotic medication (aspirin, clopidogrel, and unfractionated heparin), incubated with buffer (B) or with ALX-0081 (C) are shown. Samples were perfused over a collagen-coated surface at a wall shear rate of 1600 s⁻¹ and platelet adhesion was determined as percentage surface coverage. (D) Mean values \pm SEM for the different treatment groups (n = 8 for each treatment group).

gen is one of the most thrombogenic compounds present in the subendothelium.⁴⁴ To determine the antithrombotic potential of ALX-0081 via blocking the gpIb-VWF A1 interaction, its inhibitory effect on platelet adhesion to collagen type III at different flow rates was investigated. Anticoagulated blood, spiked with 0.8 $\mu\text{g/mL}$ ALX-0081 or buffer, was perfused over collagen type III at different shear rates and platelet deposition was measured (Figure 2A). The results clearly demonstrate that ALX-0081 prevented platelet adhesion at high-shear rates ($> 1500 \text{ s}^{-1}$) such as observed in stenosed arteries⁴⁵ and not at low-shear rates ($< 500 \text{ s}^{-1}$). Platelet adhesion experiments with washed platelets show that ALX-0081 does not interfere with the interaction of platelets to collagen under static conditions, in the absence of VWF (supplemental Figure 2). Next, different doses of ALX-0081 were spiked in anticoagulated blood and the inhibitory effect on platelet adhesion to collagen at arterial shear rates was measured (Figure 2B). Platelet adhesion was completely inhibited on spiking of $\sim 0.4 \mu\text{g/mL}$ ALX-0081.

ALX-0081 completely blocks ex vivo platelet adhesion in blood samples of patients undergoing a PCI

Perfusion studies with blood from healthy individuals or from patients undergoing a PCI procedure were performed to assess the ex vivo efficacy of ALX-0081 in combination with the standard of care treatment. In these experiments, high-shear perfusion with blood from healthy volunteers resulted in rapid and extended platelet deposition on the collagen surface (Figure 3A) with a surface coverage of $60.9\% \pm 2.9\%$ (mean \pm SEM, $n = 8$). Using blood from ACS patients treated with aspirin, clopidogrel, and unfractionated heparin, platelet aggregate size was significantly smaller ($P < .0001$; Figure 3B), with a surface coverage of $22.5\% \pm 5.3\%$ (mean \pm SEM, $n = 8$). Remarkably however, the standard of care treatment resulted in none of the patients in full inhibition of platelet function (Figures 3B,D). In contrast, addition of ALX-0081 to these samples completely and dose-dependently inhibited platelet adhesion under high-shear conditions (Figure 3C-D; surface coverage of $0.4\% \pm 0.3\%$ (mean \pm SEM, $n = 8$; $P < .0001$). For all patients, complete inhibition was observed when 0.8 $\mu\text{g/mL}$ ALX-0081 was spiked to the blood. The effective ALX-0081 dose, for example, the concentration of ALX-0081 resulting in $< 3\%$ surface coverage, ranged from 0.2 $\mu\text{g/mL}$ to 0.8 $\mu\text{g/mL}$ and was correlated to the VWF levels in the patients' plasma.⁴⁶

In vivo efficacy and safety

Because ALX-0081 is cross-reactive with baboon VWF (data not shown), the in vivo efficacy of ALX-0081 could be studied in a modified Folts model in this species.

In all animals treated with ALX-0081 ($n = 8$), a strong anti-thrombotic effect was obtained, which persisted on infusion with epinephrine (supplemental Figure 3A). Bivalency of ALX-0081 was required for its in vivo efficacy as the monovalent building block of ALX-0081, PMP12A2h1, or ALX-0081 variants in which one of the building blocks was exchanged by an irrelevant Nanobody building block, were not able to inhibit CFRs in the Folts model (data not shown). The plasma levels of ALX-0081 needed for full inhibition of CFRs in this model were between 0.3 and 0.5 $\mu\text{g/mL}$. Ex vivo RIPA analyses clearly demonstrated that complete inhibition of RIPA correlated with the observation of complete antithrombotic efficacy (Figure 4D). Therefore, RIPA can

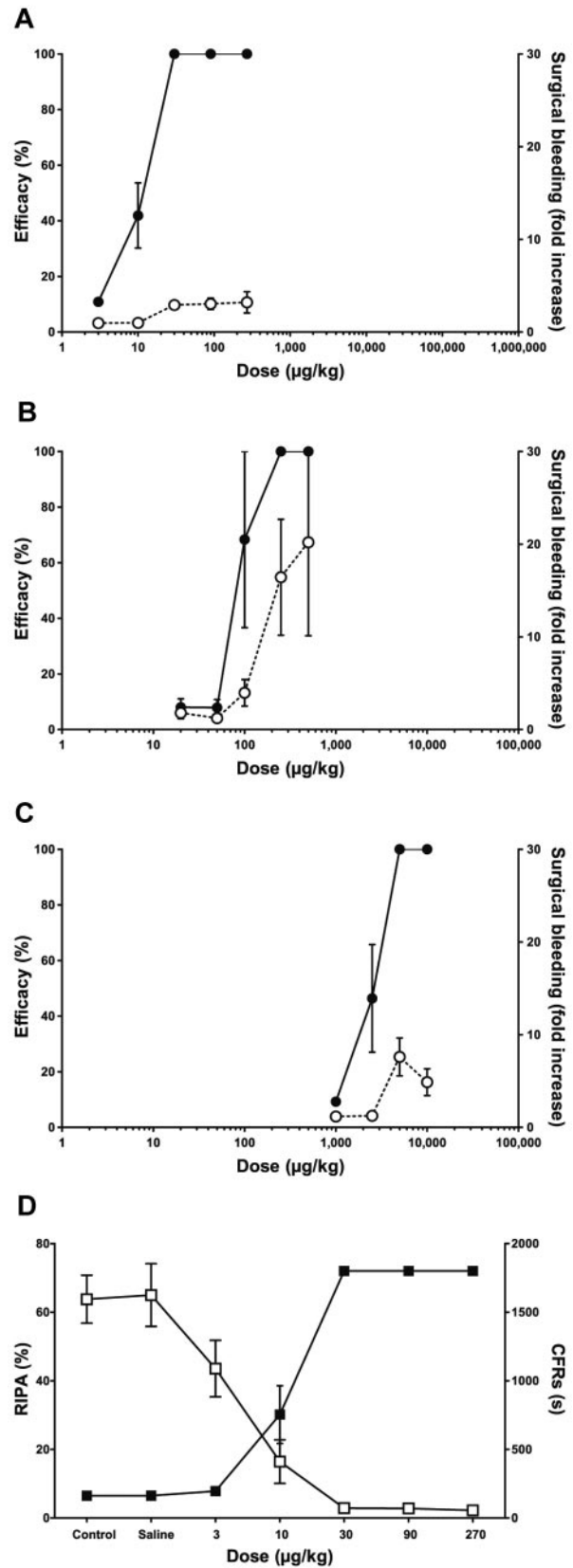


Figure 4. In vivo efficacy and safety of ALX-0081, compared with clopidogrel and abciximab. Safety (\circ , dashed lines) and efficacy (\bullet , solid lines) of ALX-0081 (A, $n = 8$), abciximab (B, $n = 3$), and clopidogrel (C, $n = 4$) are shown in function of dose in baboons. Efficacy is measured as the percentage of inhibition of CFRs in the modified Folts model and safety as n-fold increase in bleeding from a well-defined wound, compared with control levels. (D) For ALX-0081-treated animals, ex vivo RIPA measurements (\square) correlate with in vivo efficacy (\blacksquare).

be considered a good biomarker for the *in vivo* activity of ALX-0081.

Aspirin ($n = 3$) and heparin ($n = 3$) were not effective in this model (data not shown), whereas in animals treated with clopidogrel ($n = 4$), a good antithrombotic effect was observed (supplemental Figure 3C). In these latter animals, however, CFRs reappeared after infusion of epinephrine, suggesting a rather weak antithrombotic effect in this model. Abciximab inhibited thrombus formation and the effect was maintained on infusion with epinephrine ($n = 3$; supplemental Figure 3B).

The effect of ALX-0081, abciximab, and clopidogrel on bleeding was evaluated in baboons by a surgical bleeding method (Figure 4A-C). The mean blood loss from a well-defined wound was higher in animals treated with increasing doses of clopidogrel and to an even greater extent in these treated with abciximab. Blood loss in animals receiving ALX-0081 was less than in clopidogrel- and abciximab-treated animals (1.5- and 6-fold, respectively), indicating that ALX-0081 may be safer than clopidogrel and abciximab in terms of bleeding risk.

The therapeutic window of the tested compounds is reflected by the difference between the doses needed for CFR inhibition and the doses resulting in increased surgical bleeding. This dose range is larger for ALX-0081 (Figure 4A) than for abciximab (Figure 4B) and clopidogrel (Figure 4C). These results indicate that ALX-0081 has a superior therapeutic window compared with abciximab and clopidogrel in an *in vivo* efficacy and safety model in baboon.

In addition, we could also demonstrate in this animal model that the action of ALX-0081 could be reversed by VWF, suggesting that if necessary, VWF can be used as an antidote in a clinical setting (data not shown).

Finally, addition of the standard therapeutic combination of heparin, aspirin, and clopidogrel to ALX-0081 did not further enhance efficacy compared with ALX-0081 monotherapy. Moreover, addition of ALX-0081 on top of the standard antithrombotic medication did not result in an increased surgical bleeding tendency (data not shown).

Pharmacokinetics and pharmacodynamics of ALX-0081 in cynomolgus monkey

The mean observed plasma concentration time profiles as well as the mean response time plots of the percentage of RICO activity after IV bolus administration of ALX-0081 to cynomolgus monkeys are shown in Figure 5, panels A and B, respectively.

In the higher dose groups, the PK profile shows an initial phase characterized by a steep decline of total active ALX-0081 plasma levels, reflecting the clearance of free ALX-0081. This is followed by a second slower decreasing phase, reflecting the clearance of ALX-0081 bound to VWF. ALX-0081 showed a nonlinear, less than dose proportional increase in exposure. Across the different dose groups, the apparent terminal half-life ranged from 17 to 30 hours. These numbers coincide with the reported half-life for VWF in cynomolgus monkey (Table 1).

The time course of the PD effect curves corresponded very well with the temporal profile of ALX-0081 plasma concentrations in all dose groups (Figure 5B). VWF activity was neutralized immediately after administration of ALX-0081 and was sustained between 4-24 hours for the different dose groups. PK/PD analysis indicated that plasma levels exceeding $1 \mu\text{g/mL}$ ALX-0081 resulted in complete RICO inhibition.

Nonclinical and clinical PK data have been used to verify the mechanistic PK/PD model which describes clearance mechanisms

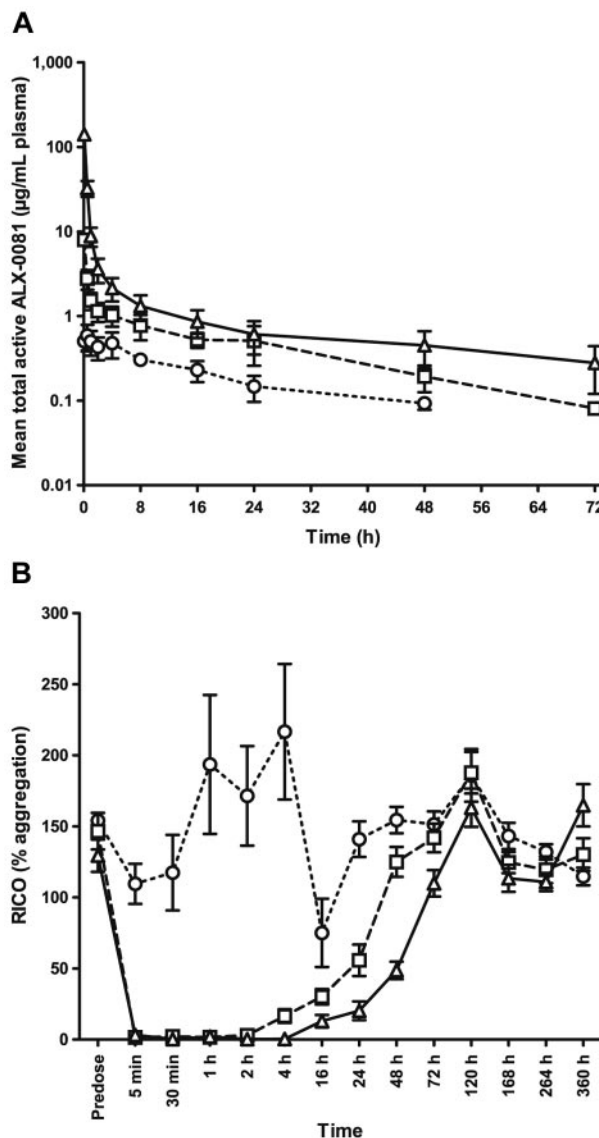


Figure 5. Pharmacokinetic and pharmacodynamic properties of ALX-0081 after single IV administration to cynomolgus monkeys. Different doses of ALX-0081 were administered as an IV bolus injection: 0.02 mg/kg (○, dotted lines), 0.40 mg/kg (□, dashed lines), or 8.00 mg/kg (△, solid lines); $n = 6$ for each dose level, except for the 8.00 mg/kg group, where one animal was considered an outlier because of a nondecreasing profile and was therefore excluded from the analysis ($n = 5$). (A) Mean (\pm SD) observed ALX-0081 plasma concentrations are shown in function of time. (B) RICO (mean \pm SEM) was determined as a measure for the inhibitory effect of ALX-0081 on VWF-mediated platelet aggregation.

and drug-target relationships of ALX-0081. The model has been used to optimize the design of further preclinical and clinical studies.

Biodistribution of ALX-0081

ALX-0081 does not bind to murine VWF and it was previously demonstrated that human and murine VWF show the same biodistribution and clearance pathways in mice.⁴⁷ Therefore, mice can serve as an elegant model to study both the biodistribution and clearance of ALX-0081, and the effects of its target, human VWF.

On IV administration of ALX-0081 alone, the majority of radioactivity was found in blood, kidneys, and liver (Figure 6A), whereas only small amounts were detected in other organs. In a time-course experiment, 80% of total radioactivity was found in

Table 1. Basic pharmacokinetic parameters for ALX-0081 after single IV administration to cynomolgus monkeys

Dose, mg/kg	AUC _{inf} , h × kg/mL	CL, mL/h/kg	t _{1/2} terminal, h
0.02	0.559 ± 0.192	1.97 ± 0.65	17.0 ± 6.6
0.40	0.085 ± 0.025	13.24 ± 6.11	18.9 ± 6.1
8.00*	0.016 ± 0.004	65.69 ± 15.31	30.2 ± 5.3

Mean ± SD, n = 6 per dose level. Increase of CL with dose is an artifact of the noncompartmental analysis.

AUC_{inf} indicates area under the plasma concentration time curve, calculated from 0 to infinity; D, dose; and CL, clearance.

*One animal was considered an outlier due to a nondecreasing profile and was therefore excluded from the analysis (n = 5).

blood immediately after IV injection. Fifteen minutes thereafter, this amount had decreased to 16%, whereas the amount in the kidneys had increased from 14% to 41%. The remaining radioactivity in blood declined slowly in the following hours.

On injection of VWF-bound ALX-0081, 75% of total radioactivity was found in blood (Figure 6B). One hour after the injection, this amount had only decreased to 50%, indicating a less rapid elimination of ALX-0081 from the circulation when bound to

VWF. The amount of radioactivity in the liver increased to 25%, whereas only 2.5% was found in the kidneys.

Taken together, the data suggest that unbound ALX-0081 is eliminated rather rapidly via the kidneys, whereas ALX-0081 bound to its target stays in circulation longer and possibly degrades via a hepatic pathway together with the carrier VWF. These results are in line with the biphasic concentration time curves observed in the cynomolgus monkey (Figure 5A).

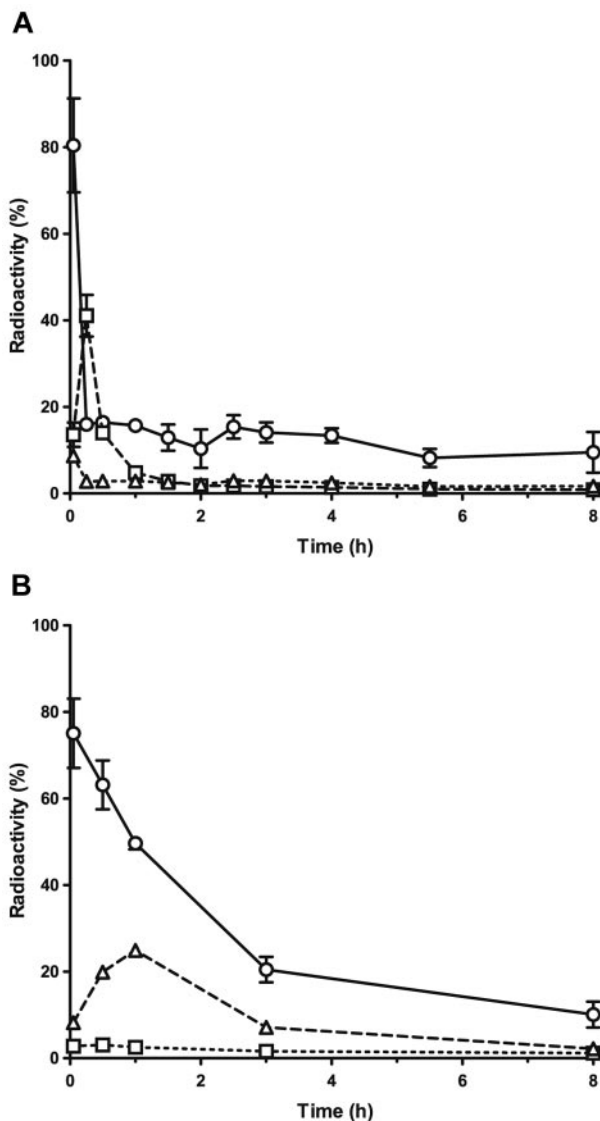


Figure 6. Biodistribution of free ALX-0081 and ALX-0081 complexed with human VWF in mice. Radioactivity (as percentage of total) found in blood (○, solid lines), kidney (□, dashed lines), and liver (△, dotted lines) on injection of ¹²⁵I-radiolabeled ALX-0081 free (A) or in complex with human VWF (B). Results are expressed as mean ± SD, n = 3 for each time point.

Discussion

Current strategies to prevent thrombotic events during and after angioplasty procedures include the use of platelet aggregation inhibitors such as aspirin, clopidogrel, and gpIIb/IIIa inhibitors (eg, abciximab). An important common feature of these drugs is their indiscriminate mode of action: they interfere with hemostasis and clot formation throughout the entire cardiovascular system, irrespective of the blood shear rate. Consequently, their use is associated with an increased occurrence of bleeding complications, including bleeding at catheterization sites, gastrointestinal bleeding, and cerebral hemorrhage.^{1,2} This safety hurdle also puts a limit to their efficacy because it implies that only suboptimal doses can be administered to treat thrombosis without seriously affecting normal hemostasis. Moreover, a significant proportion of patients show resistance to aspirin and/or clopidogrel, further limiting the applicability of both drugs.⁴

Taken together, there is a clear medical need for a selective, potent and safe antithrombotic drug. Here we describe the mode of action and the preclinical PK, PD, and safety profile of ALX-0081, a novel antithrombotic Nanobody.

Nanobodies are based on the smallest functional fragments of single-chain Abs and can therefore easily be formatted in multivalent or multispecific constructs to tailor their binding properties. For ALX-0081, we clearly demonstrated that combining 2 identical monovalent VWF-binding Nanobodies into 1 bivalent Nanobody significantly improved binding avidity. Furthermore, this also translated into an enhanced in vitro potency, reflected by the inhibitory effect of ALX-0081 on VWF binding to platelets.

ALX-0081 specifically targets the VWF A1 domain, which is involved very early in the process of thrombus formation. VWF only interacts with the platelet gpIb receptor through its A1 domain under high-shear conditions,^{8,9} suggesting a more selective mode of action for anti-VWF compounds like ALX-0081. Indeed, the results from in vitro perfusion chamber experiments clearly demonstrate that ALX-0081 selectively inhibits platelet adhesion to collagen at high-shear rates (> 1500 s⁻¹), such as observed in normal arterioles and stenotic arteries.⁴⁵

Because ACS patients undergoing elective PCI are the primary target population for early clinical trials with ALX-0081, blood samples of these patients were used to evaluate the in vitro

antithrombotic activity of ALX-0081. Whereas the standard-of-care treatment (consisting of aspirin, heparin and clopidogrel) only resulted in partial inhibition of platelet adhesion to collagen, this inhibition was complete after the addition of ALX-0081. It is important to note that the effective concentration of ALX-0081 in these ex vivo experiments depended on the VWF concentration in the plasma samples. VWF levels are generally higher in ACS patients,^{48,49} explaining the higher effective concentration of ALX-0081 needed to achieve full effect in samples from this patient population (~ 0.8 µg/mL) compared with healthy individuals (~ 0.4 µg/mL).

Efficacy of ALX-0081 was further investigated in vivo in a baboon Folts model for ACS and stable angina. The ALX-0081 plasma levels needed for full inhibition of CFRs in vivo (0.3-0.5 µg/mL) corresponded well to the effective concentration of ALX-0081 in the ex vivo experiments. Furthermore, the in vivo efficacy data support the excellent in vitro potency demonstrated for ALX-0081: only ALX-0081 and abciximab were able to completely abolish the CFRs, even after infusion of epinephrine, a potent stimulator of platelet activation. Ten-fold lower doses of ALX-0081 were needed to obtain the same effect as abciximab.

Not only efficacy, but also safety of ALX-0081 compared favorably to that of other antithrombotics. Surgical bleeding was significantly lower in animals receiving ALX-0081 than in animals receiving clopidogrel or abciximab. Together, the lower effective dose and the lower bleeding risk clearly indicate that ALX-0081 has a broader therapeutic window than the currently marketed antithrombotic drugs clopidogrel and abciximab.

Finally, ALX-0081 shows favorable PK properties, as demonstrated in the cynomolgus monkey as a cross-reactive species and in radiolabel experiments with human VWF in mice. ALX-0081 bound to its target VWF stays in circulation with an apparent half-life of 17-30 hours in cynomolgus monkeys and most likely is degraded via a hepatic pathway, similar to free VWF.⁴⁷ Unbound excess ALX-0081 is cleared rapidly via the kidneys, thus limiting the risk for undue drug accumulation or overdosing. After IV administration in cynomolgus monkeys a biphasic concentration time curve can be described. An initial phase characterized by a steep decline of total active ALX-0081 in plasma could be explained by rapid renal elimination of excess of drug. A second slower decreasing phase could be attributed to ALX-0081 in complex with VWF. The reported half-life of VWF for cynomolgus monkey coincides with the apparent half-life of the described second phase. However, results from noncompartmental analysis have to be interpreted with caution, especially in case of molecules which exhibit complex PK behavior like many protein drugs. Therefore a 3-compartmental semimechanistic PK model has been developed that can accurately describe the PK and PD properties of ALX-0081. From that it becomes apparent that indeed 2 distinct clearance rates account for the overall disposition which can be assigned to a target independent mechanism on the one hand and a target dependent mechanism on the other hand. The resulting

favorable half-life is expected to support convenient dosing regimens in humans.

Because VWF is the target of ALX-0081 and VWF acts as a carrier for FVIII, plasma levels of both proteins were monitored on single IV administration of ALX-0081 to cynomolgus monkeys. Variable plasma levels were observed for all treated and control animals. The single-dose setup of the study did not allow to draw clear conclusions on the possible effects of ALX-0081 on VWF and FVIII plasma levels. However, observed decreases in VWF and FVIII levels were never symptomatic (data not shown).

Building on this extensive and convincing preclinical data package and subsequent toxicology studies, two phase 1 clinical trials have been successfully completed^{32,33} and a phase 2 trial in high-risk PCI patients comparing the efficacy and safety of ALX-0081 to abciximab is currently ongoing.

Acknowledgments

The authors thank Alex Hemeryck, Sven Hoefman, Stefan de Buck, Torsten Dreier, and all other (former) collaborators at Ablynx for their contribution to the ALX-0081 project; Philip De Groot and colleagues (UMC Utrecht, Utrecht, The Netherlands) for assistance with the platelet aggregation and adhesion assays; and Dr Cécile Denis and Dr Peter Lenting (both Inserm U770, France) for performing biodistribution experiments in mice. We are also grateful to the research groups of Frank Leebeek (EMC Rotterdam, Rotterdam, The Netherlands) and Philip Badenhorst (University of the Free State, Bloemfontein, South Africa) for the collaboration on the ex vivo platelet aggregation experiments and the baboon studies, respectively.

Authorship

Contribution: H.U. designed research, performed research, analyzed and interpreted data, and wrote the manuscript; K.S., A.S., P.d.J., J.R., S.P., M.L., and P.C. designed research, performed research, and analyzed and interpreted data; S.R. and F.V.B. analyzed and interpreted data, and wrote the manuscript; K.V. analyzed and interpreted data, and performed statistical analysis; P.S. and J.-B.H. designed research; and J.B. designed research, and analyzed and interpreted data.

Conflict-of-interest disclosure: H.U., A.S., S.R., S.P., P.C., F.V.B., K.V., P.S., J.B., and J.-B.H. are employees of Ablynx NV. K.S. and M.L. are former employees of Ablynx NV. H.U., A.S., S.P., M.L., P.C., F.V.B., K.V., P.S., J.B., and J.-B.H. own shares and/or stock options of Ablynx NV. The remaining authors declare no competing financial interests.

Nanobody is a registered trademark of Ablynx NV.

Correspondence: Hans Ulrichs, Ablynx NV, Technologiepark 21, B-9052 Zwijnaarde, Belgium; e-mail: Hans.Ulrichs@ablynx.com.

References

- Bhatt DL, Topol EJ. Scientific and therapeutic advances in antiplatelet therapy. *Nat Rev Drug Discov*. 2003;2(1):15-28.
- Jackson SP, Schoenwaelder SM. Antiplatelet therapy: in search of the 'magic bullet'. *Nat Rev Drug Discov*. 2003;2(10):775-789.
- Herbert JM, Dol F, Bernat A, Falotico R, Lale A, Savi P. The antiaggregating and antithrombotic activity of clopidogrel is potentiated by aspirin in several experimental models in the rabbit. *Thromb Haemost*. 1998;80(3):512-518.
- Michos ED, Ardehali R, Blumenthal RS, Lange RA, Ardehali H. Aspirin and clopidogrel resistance. *Mayo Clin Proc*. 2006;81(4):518-526.
- Miura S, Li CQ, Cao Z, Wang H, Wardell MR, Sadler JE. Interaction of von Willebrand factor domain A1 with platelet glycoprotein Ibalpha-(1-289). Slow intrinsic binding kinetics mediate rapid platelet adhesion. *J Biol Chem*. 2000; 275(11):7539-7546.
- Sixma JJ, Schiphorst ME, Verweij CL, Pannekoek H. Effect of deletion of the A1 domain of von Willebrand factor on its binding to heparin, collagen and platelets in the presence of ristocetin. *Eur J Biochem*. 1991;196(2):369-375.
- Spiel AO, Gilbert JC, Jilma B. von Willebrand factor in cardiovascular disease: focus on acute

- coronary syndromes. *Circulation*. 2008;117(11):1449-1459.
8. Ikeda Y, Handa M, Kawano K, et al. The role of von Willebrand factor and fibrinogen in platelet aggregation under varying shear stress. *J Clin Invest*. 1991;87(4):1234-1240.
 9. Peterson DM, Stathopoulos NA, Giorgio TD, Hellums JD, Moake JL. Shear-induced platelet aggregation requires von Willebrand factor and platelet membrane glycoproteins Ib and IIb/IIIa. *Blood*. 1987;69(2):625-628.
 10. Andre P, Hainaud P, Bal dit SC, Garfinkel LI, Caen JP, Drouet LO. Relative involvement of GPIIb/IX-vWF axis and GPIIb/IIIa in thrombus growth at high shear rates in the guinea pig. *Arterioscler Thromb Vasc Biol*. 1997;17(5):919-924.
 11. Kawasaki T, Kaku S, Kohinata T, et al. Inhibition by aurointricarboxylic acid of von Willebrand factor binding to platelet GPIIb, platelet retention, and thrombus formation in vivo. *Am J Hematol*. 1994;47(1):6-15.
 12. Strony J, Phillips M, Brands D, Moake J, Adelman B. Aurintricarboxylic acid in a canine model of coronary artery thrombosis. *Circulation*. 1990;81(3):1106-1114.
 13. Azzam K, Garfinkel LI, Bal dit SC, Cisse TM, Drouet L. Antithrombotic effect of a recombinant von Willebrand factor, VCL, on nitrogen laser-induced thrombus formation in guinea pig mesenteric arteries. *Thromb Haemost*. 1995;73(2):318-323.
 14. Gurevitz O, Goldfarb A, Hod H, et al. Recombinant von Willebrand factor fragment AR545C inhibits platelet aggregation and enhances thrombolysis with rPA in a rabbit thrombosis model. *Arterioscler Thromb Vasc Biol*. 1998;18(2):200-207.
 15. McGhie AI, McNatt J, Ezov N, et al. Abolition of cyclic flow variations in stenosed, endothelium-injured coronary arteries in nonhuman primates with a peptide fragment (VCL) derived from human plasma von Willebrand factor-glycoprotein Ib binding domain. *Circulation*. 1994;90(6):2976-2981.
 16. Yao SK, Ober JC, Garfinkel LI, et al. Blockade of platelet membrane glycoprotein Ib receptors delays intracoronary thrombogenesis, enhances thrombolysis, and delays coronary artery reocclusion in dogs. *Circulation*. 1994;89(6):2822-2828.
 17. Hennen JK, Swillo RE, Morgan GA, et al. Pharmacologic inhibition of platelet vWF-GPIIb alpha interaction prevents coronary artery thrombosis. *Thromb Haemost*. 2006;95(3):469-475.
 18. Wadanoli M, Sako D, Shaw GD, et al. The von Willebrand factor antagonist (GPG-290) prevents coronary thrombosis without prolongation of bleeding time. *Thromb Haemost*. 2007;98(2):397-405.
 19. Bellinger DA, Nichols TC, Read MS, et al. Prevention of occlusive coronary artery thrombosis by a murine monoclonal antibody to porcine von Willebrand factor. *Proc Natl Acad Sci U S A*. 1987;84(22):8100-8104.
 20. Cadroy Y, Hanson SR, Kelly AB, et al. Relative antithrombotic effects of monoclonal antibodies targeting different platelet glycoprotein-adhesive molecule interactions in nonhuman primates. *Blood*. 1994;83(11):3218-3224.
 21. Kageyama S, Yamamoto H, Nagano M, Arisaka H, Kayahara T, Yoshimoto R. Anti-thrombotic effects and bleeding risk of AjvW-2, a monoclonal antibody against human von Willebrand factor. *Br J Pharmacol*. 1997;122(1):165-171.
 22. Kageyama S, Yamamoto H, Yoshimoto R. Anti-human von willebrand factor monoclonal antibody AjvW-2 prevents thrombus deposition and neointima formation after balloon injury in guinea pigs. *Arterioscler Thromb Vasc Biol*. 2000;20(10):2303-2308.
 23. Kageyama S, Yamamoto H, Nakazawa H, Yoshimoto R. Anti-human vWF monoclonal antibody, AjvW-2 Fab, inhibits repetitive coronary artery thrombosis without bleeding time prolongation in dogs. *Thromb Res*. 2001;101(5):395-404.
 24. Kageyama S, Yamamoto H, Nakazawa H, et al. Pharmacokinetics and pharmacodynamics of AJW200, a humanized monoclonal antibody to von Willebrand factor, in monkeys. *Arterioscler Thromb Vasc Biol*. 2002;22(1):187-192.
 25. Kageyama S, Matsushita J, Yamamoto H. Effect of a humanized monoclonal antibody to von Willebrand factor in a canine model of coronary arterial thrombosis. *Eur J Pharmacol*. 2002;443(1-3):143-149.
 26. Krupski WC, Bass A, Cadroy Y, Kelly AB, Harker LA, Hanson SR. Antihemostatic and antithrombotic effects of monoclonal antibodies against von Willebrand factor in nonhuman primates. *Surgery*. 1992;112(2):433-439.
 27. Yamamoto H, Vreys I, Stassen JM, Yoshimoto R, Vermeylen J, Hoylaerts MF. Antagonism of vWF inhibits both injury induced arterial and venous thrombosis in the hamster. *Thromb Haemost*. 1998;79(1):202-210.
 28. Diener JL, Daniel Lagasse HA, Duerschmied D, et al. Inhibition of von Willebrand factor-mediated platelet activation and thrombosis by the anti-von Willebrand factor A1-domain aptamer ARC1779. *J Thromb Haemost*. 2009;7(7):1155-1162.
 29. Gurevitz O, Eldar M, Skutelsky E, et al. S-nitrosoderivative of a recombinant fragment of von Willebrand factor (S-nitroso-AR545C) inhibits thrombus formation in guinea pig carotid artery thrombosis model. *Thromb Haemost*. 2000;84(5):912-917.
 30. Gilbert JC, DeFeo-Fraulini T, Hutabarat RM, et al. First-in-human evaluation of anti von Willebrand factor therapeutic aptamer ARC1779 in healthy volunteers. *Circulation*. 2007;116(23):2678-2686.
 31. Machin S, Clarke C, Ikemura O, et al. A humanized monoclonal antibody against vWF A1 domain inhibits vWF: R1Cof activity and platelet adhesion in human volunteers [abstract]. *J Thromb Haemost*. 2003;(suppl 1):Abstract OC328.
 32. Bartunek J, Barbato E, Verduyck K, et al. Safety and efficacy of anti-von Willebrand factor Nanobody ALX-0081 in stable angina patients undergoing percutaneous coronary intervention [abstract]. *Circulation*. 2010;122:Abstract 15084.
 33. Bartunek J, Barbato E, Holz J-B, Verduyck K, Ulrichs H, Heyndrickx G. ALX-0081 a novel anti-thrombotic: results of a single-dose phase 1 study in healthy volunteers and further development in patients with stable angina [abstract]. *Circulation*. 2008;118:Abstract 2009.
 34. Hamers-Casterman C, Atarhouch T, Muyldermans S, et al. Naturally occurring antibodies devoid of light chains. *Nature*. 1993;363(6428):446-448.
 35. Van Bockstaele F, Holz J-B, Revets H. The development of nanobodies for therapeutic applications. *Curr Opin Investig Drugs*. 2009;10(11):1212-1224.
 36. Yao SK, McNatt J, Cui K, et al. Combined ADP and thromboxane A2 antagonism prevents cyclic flow variations in stenosed and endothelium-injured arteries in nonhuman primates. *Circulation*. 1993;88(6):2888-2893.
 37. Folts J. An in vivo model of experimental arterial stenosis, intimal damage, and periodic thrombosis. *Circulation*. 1991;83(6 suppl):IV3-IV14.
 38. Fontayne A, Meiring M, Lamprecht S, et al. The humanized anti-glycoprotein Ib monoclonal antibody h6B4-Fab is a potent and safe antithrombotic in a high shear arterial thrombosis model in baboons. *Thromb Haemost*. 2008;100(4):670-677.
 39. Wu D, Meiring M, Kotze HF, Deckmyn H, Cauwenberghs N. Inhibition of platelet glycoprotein Ib, glycoprotein IIb/IIIa, or both by monoclonal antibodies prevents arterial thrombosis in baboons. *Arterioscler Thromb Vasc Biol*. 2002;22(2):323-328.
 40. Wu D, Vanhoorelbeke K, Cauwenberghs N, et al. Inhibition of the von Willebrand (VWF)-collagen interaction by an antihuman VWF monoclonal antibody results in abolition of in vivo arterial platelet thrombus formation in baboons. *Blood*. 2002;99(10):3623-3628.
 41. Anfossi G, Trovati M. Role of catecholamines in platelet function: pathophysiological and clinical significance. *Eur J Clin Invest*. 1996;26(5):353-370.
 42. Benedict CR, Ryan J, Wolitzky B, et al. Active site-blocked factor IXa prevents intravascular thrombus formation in the coronary vasculature without inhibiting extravascular coagulation in a canine thrombosis model. *J Clin Invest*. 1991;88(5):1760-1765.
 43. Thiagarajan P, Benedict CR. Inhibition of arterial thrombosis by recombinant annexin V in a rabbit carotid artery injury model. *Circulation*. 1997;96(7):2339-2347.
 44. van Zanten GH, de GS, Slootweg PJ, et al. Increased platelet deposition on atherosclerotic coronary arteries. *J Clin Invest*. 1994;93(2):615-632.
 45. Kroll MH, Hellums JD, McIntire LV, Schafer AI, Moake JL. Platelets and shear stress. *Blood*. 1996;88(5):1525-1541.
 46. van Loon J, de Jaegere P, Ulrichs H, et al. The in vitro effect of the new antithrombotic drug candidate ALX-0081 on blood samples of patients undergoing PCI [published online ahead of print June 9, 2011]. *Thromb Haemost*. doi:10.1160/TH10-12-0804.
 47. Lenting PJ, Westein E, Terraube V, et al. An experimental model to study the in vivo survival of von Willebrand factor. Basic aspects and application to the R1205H mutation. *J Biol Chem*. 2004;279(13):12102-12109.
 48. Gorog DA, Douglas H, Ahmed N, Lefroy DC, Davies GJ. Coronary angioplasty enhances platelet reactivity through von Willebrand factor release. *Heart*. 2003;89(3):329-330.
 49. Sakai H, Goto S, Kim JY, et al. Plasma concentration of von Willebrand factor in acute myocardial infarction. *Thromb Haemost*. 2000;84(2):204-209.